1991년도 봄
한국전산구조공학회 학술발표회 논문집

해양구조물의 파력산정을 위한 3-차원 무한요소

THREE-DIMENSIONAL INFINITE ELEMENTS FOR WAVE FORCE EVALUATION ON OFFSHORE STRUCTURES

박 우 선　　윤 정 방　　편 종 근

Park, Woo-Sun* Yun, Chung-Bang† and Pyun, Chong-Kun‡

Abstract

The finite element technique incorporating infinite elements is applied to analyzing the general three dimensional wave–structure interaction problems within the limits of linear wave theory. The hydrodynamic forces are assumed to be inertially dominated, and viscous effects are neglected. In order to analyze the corresponding boundary value problems efficiently, two types of elements are developed. One is the infinite element for modeling the radiation condition at infinity, and the other is the fictitious bottom boundary element for the case of deep water. To validate those elements, numerical analyses are performed for several floating structures. Comparisons with the results from other available solution methods show that the present method incorporating the infinite and the fictitious bottom boundary elements gives good results.

1. Introduction

The linear wave diffraction theory is commonly used to evaluate the hydrodynamic forces on large offshore structures. In general, there are two types of numerical solution techniques for the corresponding boundary value problems. They are the boundary integral equation method (BIEM) and the finite element method (FEM). The boundary integral equation formulations are more frequently adopted. However, the methods fail at so-called critical or irregular frequencies[1], and are more difficult to be applied to the cases with complex structural geometries such as sharp corners. Therefore, the interest in the alternative approaches inbased on the finite element method has been increased considerably.

Application of the finite element method to the evaluation of hydrodynamic forces on large offshore structures have been extensively reviewed by Mei[2] and by Zienkiewicz *et al.*[3]. There are mainly four different approaches which have been adopted in the finite element method to model the radiation condition at infinity. They are (1) boundary damper applied along the outer boundary at finite distance from the submerged solid body of interest[4-8], (2) matching analytical boundary series solutions[9-12], (3) matching boundary integral solutions[9,12,13], and (4) infinite elements[14-17]. The methods (2) and (3) are commonly referred as the hybrid element method (HEM) or the localized finite element method (LFEM). The concept of an infinite element has been adopted in this study.

Bettess and Zienkiewicz[14] firstly applied a two dimensional infinite element with exponential decay to the horizontal plane problems of surface waves. Later, Zienkiewicz *et al.*[15] presented a new infinite element with $r^{-1/2}$ decay, which is also a horizontal two dimensional element. It was reported that this element gives more accurate results than the infinite element with exponential decay and any boundary damper elements. Lau and Ji[16] suggested a three dimensional 8-noded infinite element using the first two terms of asymptotic expansions of the progressive wave component in the analytical boundary series solutions to construct the shape functions in the radial direction. It was shown that the element gives satisfactory results for the fixed cases (i.e., diffraction problems), compared with those by using the matching boundary series solutions. However, this element may be improper to the wave radiation problems, since the element does not include the effects of evanescent wave components (standing wave components or local disturbance terms) which may be significant. Recently, an axisymmetric infinite element was developed by the present authors[17], which can be applicable to the boundary value problems for the vertical axisymmetric structures. The shape functions for the element, in the radial direction, were derived from

*Senior Researcher, Ocean Engineering Lab., KORDI
†Professor, Dept. of Civil Engineering, KAIST
‡Professor, Dept. of Civil Engineering, Myong Ji Univ.

the asymptotic expressions for the progressive wave and the first evanescent wave components in the analytical boundary series solutions. The efficiency and validity of the element have been proved through the example analyses for the various cases of the vertical axisymmetric structures.

In this study, the axisymmetric infinite element developed in the previous study[17] is expanded to be applicable to the general three dimensional wave–structure interaction problems. The fictitious bottom boundary element is also introduced in order to analyze the boundary value problems in deep water, efficiently. To validate the infinite and the fictitious bottom boundary elements, the numerical analysis is performed for several cases of the floating structures. Comparisons with the results obtained by other available solution methods show that the present method incorporating the infinite and the fictitious bottom boundary elements gives good results.

2. Governing equation and boundary conditions

In this study, a regular wave train of amplitude, ζ_a, and angular frequency, ω, propagating in water of constant depth, d, and passing a floating arbitrary shaped body is considered, as shown in *Figure 1*. A Cartesian coordinate system (x, y, z) with z measured vertically upwards from the still water level is adopted. Also, a cylindrical coordinate system (r, θ, z) is employed with r measured radially from the z axis, and θ from the positive x axis. The fluid is assumed to be incompressible and inviscid, and the flow is irrotational. The fluid motion, therefore, can be described by a scalar velocity potential, $\Phi(x, y, z; t)$, which satisfies the Laplace equation

$$\nabla^2\Phi(x, y, z; t) = 0 \tag{1}$$

The wave height is assumed to be sufficiently small for linear wave theory to be applied. Consequently, Φ is subjected to the usual boundary conditions at the seabed(S_d), body surface(S_b), and free surface(S_f) as follows.

$$\frac{\partial\Phi}{\partial z} = 0; \quad \text{on } S_d \tag{2}$$

$$\frac{\partial\Phi}{\partial z} = \frac{\omega^2}{g}\Phi; \quad \text{on } S_f \tag{3}$$

$$\frac{\partial\Phi}{\partial n} = V_n; \quad \text{on } S_b \tag{4}$$

in which n = the outward unit normal to the body surface, S_b; and V_n = the velocity of the body surface itself in the direction normal to the surface; i.e., n.

A wave train will cause the body to oscillate in the six modes corresponding to surge, sway, heave, roll, pitch, and yaw as indicated in *Figure 2*, and denoted here by subscripts 1, 2, 3, 4, 5, and 6, respectively. Each mode of motion is assumed to be harmonic and

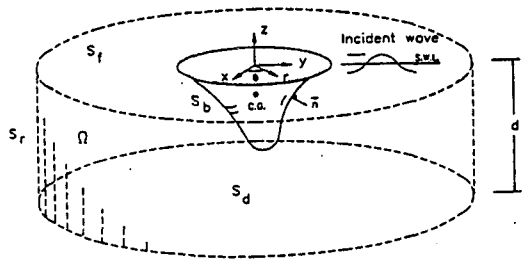

Figure 1 Definition sketch

expressed in the form of $\xi_j e^{-i\omega t}$ in which t = time, and ξ_j = the corresponding complex valued amplitude. Therefore, V_n is itself made up of surge, sway, heave, roll, pitch, and yaw components, and is given as

$$V_n = \mathrm{Re}[\sum_{j=1}^{6} -i\omega n_j \xi_j e^{-i\omega t}] \tag{5}$$

in which Re[·] denotes the real part of the argument, $i = \sqrt{-1}$, and

$$\begin{aligned} n_1 &= n_x; \quad n_2 = n_y; \quad n_3 = n_z; \\ n_4 &= (y - y_g)n_z - (z - z_g)n_y; \\ n_5 &= (z - z_g)n_x - (x - x_g)n_z; \\ n_6 &= (x - x_g)n_y - (y - y_g)n_x \end{aligned} \tag{6}$$

and n_x, n_y, n_z = the direction cosines of the outward normal vector, $\bar{n}$, to the body surface with respect to the x, y, and z directions, respectively; and x_g, y_g, z_g = the coordinates of the center of gravity of the body.

The velocity potential, Φ, is also harmonic and is made up of components associated with the incident wave(subscript 0), the diffracted waves(subscript 7), and the radiated waves due to each motion(subscript $1, 2, \cdots, 6$). Then, Φ may be expressed in the usual way as

$$\Phi = \mathrm{Re}[(\phi_0 + \phi_7 + \sum_{j=1}^{6} \phi_j \xi_j) e^{-i\omega t}] \tag{7}$$

in which the velocity potential, ϕ_j, is generally a complex valued quantity. The velocity potentials associated with the diffracted and radiated waves must satisfy the Sommerfeld radiation condition at infinity[18].

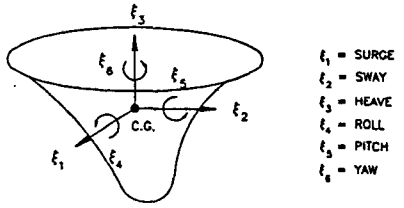

Figure 2 Definition of body motions

$$\lim_{r\to\infty}\sqrt{r}\left(\frac{\partial\phi_j}{\partial r}-ik_0\phi_j\right) = 0 \qquad (8)$$

in which k_0 = the wave number.

Substituting equations (5)–(6) into equation (4), and separating out the terms corresponding to the diffraction problem($j = 0,7$) and those related to the radiation problem($j = 1,2,\cdots,6$), the body surface boundary condition can be expressed as

$$\frac{\partial\phi_j}{\partial n} = \begin{cases} -i\omega n_j & \text{for } j = 1,\cdots,6 \\ -\frac{\partial\phi_0}{\partial x}n_x - \frac{\partial\phi_0}{\partial y}n_y - \frac{\partial\phi_0}{\partial z}n_z & \text{for } j = 7 \end{cases} \qquad (9)$$

in which ϕ_0 is the incident wave potential given by

$$\phi_0 = -i\frac{g\zeta_a}{\omega}\frac{\cosh[k_0(z+d)]}{\cosh(k_0 d)}e^{ik_0(x\cos\psi+y\sin\psi)} \qquad (10)$$

and ψ = the angle of wave attack measured from the positive x–axis.

3. Functional

Solution for the boundary value problems mentioned in the previous section may be obtained using the finite element method (FEM). Using the calculus of variations, the solution to the problems described in equations (1)–(3), (8), and (9) can be taken as the potential which minimizes the following functional corresponding to the governing equation and the associated boundary conditions:

$$\begin{aligned}\Pi(\phi_j) &= \int_\Omega \frac{1}{2}\nabla\phi_j\cdot\nabla\phi_j\, d\Omega \\ &- \int_{S_f}\frac{1}{2}\frac{\omega^2}{g}(\phi_j)^2 dS_f \\ &- \int_{S_r}\frac{1}{2}ik_0(\phi_j)^2 dS_r \\ &+ \int_{S_b}\frac{\partial\phi_j}{\partial n}\phi_j\, dS_b \end{aligned} \qquad (11)$$

in which Ω, S_f, S_r, and S_b denote the fluid domain, the free surface taken along $z = 0$, the radiation boundary surface at infinity, and the body surface, respectively.

To model the fluid domain efficiently, it is divided into two regions: Ω_1 is the inner finite element region surrounding the solid body with the outer cylindrical boundary surface at finite distance, r_a, from the origin, and Ω_2 is the infinite element region outside of Ω_1, as shown in *Figure 3*. For the convenience of the finite element formulation, the functionals for the finite element region are defined by using the Cartesian coordinate system, while those for the infinite element region are defined by using the cylindrical coordinate system, which are represented as

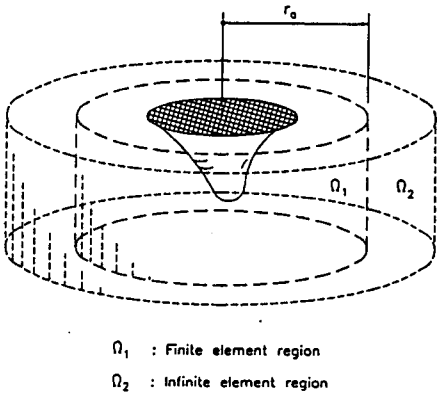

Figure 3 Division of fluid domain

o Finite element region:

$$\begin{aligned}\Pi(\phi_j) &= \int_{\Omega_1}\frac{1}{2}[(\frac{\partial\phi_j}{\partial x})^2+(\frac{\partial\phi_j}{\partial y})^2+(\frac{\partial\phi_j}{\partial z})^2]d\Omega_1 \\ &- \int_{S_f}\frac{1}{2}\frac{\omega^2}{g}(\phi_j)^2 dS_f \\ &+ \int_{S_b}\frac{\partial\phi_j}{\partial n}\phi_j\, dS_b \end{aligned} \qquad (12)$$

o Infinite element region:

$$\begin{aligned}\Pi(\phi_j) &= \int_{\Omega_2}\frac{1}{2}[(\frac{\partial\phi_j}{\partial r})^2+\frac{1}{r^2}(\frac{\partial\phi_j}{\partial\theta})^2+(\frac{\partial\phi_j}{\partial z})^2]d\Omega_2 \\ &- \int_{S_f}\frac{1}{2}\frac{\omega^2}{g}(\phi_j)^2 dS_f \\ &- \int_{S_r}\frac{1}{2}ik_0(\phi_j)^2 dS_r \end{aligned} \qquad (13)$$

4. Discretization of fluid domain

To discretize the problem in the standard finite element manner, it is necessary to describe the unknown potential, ϕ_j^e, for an element (e) in terms of the nodal parameter vector, $\{\phi_j^e\}$, and the prescribed shape function vector, $\{N^e\}$, as follows.

$$\phi_j^e = \{N^e\}^T\{\phi_j^e\} \qquad (14)$$

The functional is now minimized with respect to the nodal values $\{\phi_j\}$, which gives

$$\frac{\partial\Pi(\{\phi_j\})}{\partial(\{\phi_j\})} = \sum_e\left([K_j^e]\{\phi_j^e\}-\{P_j^e\}\right) = \{0\} \qquad (15)$$

in which $[K_j^e]$ is the element system matrix represented as

o Finite element region:

$$[K_j^e] = \int_{\Omega_1^e}[\{\frac{\partial N^e}{\partial x}\}\{\frac{\partial N^e}{\partial x}\}^T + \{\frac{\partial N^e}{\partial y}\}\{\frac{\partial N^e}{\partial y}\}^T + \{\frac{\partial N^e}{\partial z}\}\{\frac{\partial N^e}{\partial z}\}^T]d\Omega_1^e - \int_{S_f^e}\frac{\omega^2}{g}\{N^e\}\{N^e\}^T dS_f^e \quad (16)$$

o Infinite element region:

$$[K_j^e] = \int_{\Omega_2^e}[\{\frac{\partial N^e}{\partial r}\}\{\frac{\partial N^e}{\partial r}\}^T + \frac{1}{r^2}\{\frac{\partial N^e}{\partial \theta}\}\{\frac{\partial N^e}{\partial \theta}\}^T + \{\frac{\partial N^e}{\partial z}\}\{\frac{\partial N^e}{\partial z}\}^T]d\Omega_2^e - \int_{S_f^e}\frac{\omega^2}{g}\{N^e\}\{N^e\}^T dS_f^e - \int_{S_r^e} ik_0\{N^e\}\{N^e\}^T dS_r^e \quad (17)$$

and $\{P_j^e\}$ is given by

$$\{P_j^e\} = -\int_{S_b^e}\frac{\partial \phi_j}{\partial n}\{N^e\}dS_b^e \quad (18)$$

All of such element equations are assembled to produce a set of global equations pertaining to the fluid region. These can be written in matrix form as

$$[K_j]\{\phi_j\} = \{P_j\} \quad (19)$$

The matrix $[K_j]$ is symmetric and banded, with its half-bandwidth corresponding to the interaction between each node and its immediate neighbors.

Finite element region

For the efficient modeling, the inner region, Ω_1, is divided into the upper and the lower regions. The upper region is containing the solid body, and it is discretized by using two isoparametric elements; i.e., 20-noded brick element and 8-noded plane element as shown in *Figure 4*. The Lagrange polynomials are used for shape functions of the isoparametric elements. The lower region is modeled by using the fictitious bottom boundary elements (FBBE) as shown in *Figure 5*. The FBBE is a 8-noded element with the shape functions as

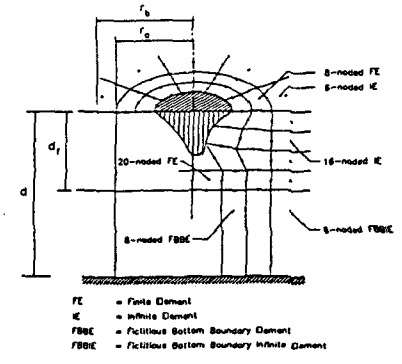

Figure 4 Modeling of fluid region

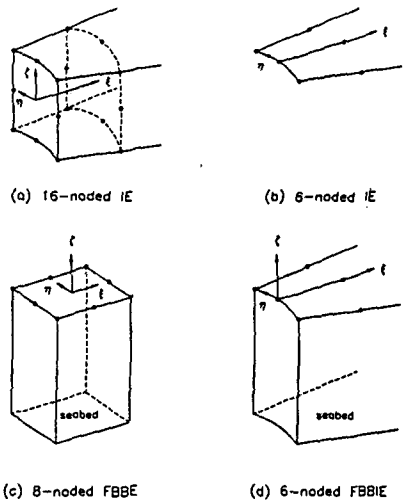

Figure 5 Definition of element coordinate systems

$$\{N^e\} = \frac{\cosh[k_0(d-d_f)(1+\zeta)]}{\cosh[k_0(d-d_f)]}\{\bar{N}(\xi,\eta)\} \quad (20)$$

with $-1 \le \xi, \eta \le 1$ and $-1 \le \zeta \le 0$, in which $\{\bar{N}(\xi,\eta)\}$ = the vector of the Lagrange shape functions and d_f = the distance from the sea water level to the top of the FBBE's. Equation (20) has been derived from the z-directional behavior of the progressive wave component in the analytical boundary series solutions, which is approximately expressed as

$$\phi_j \propto \cosh[k_0(z+d)] \quad (21)$$

The system matrices of the two isoparametric elements for the upper region are constructed using Gauss quadrature. On the other hand, the system matrices of the FBBE's are constructed by performing the integration in the ζ-direction analytically,.

Infinite element region

In order to model the radiation condition at infinity efficiently, and to avoid extensive fluid domain discretizations for the case of deep water, the three types of infinite elements are developed. They are 16-noded and 6-noded infinite elements (IE), and a 6-noded fictitious bottom boundary infinite element (FBBIE) shown in *Figure 5*. As shown in *Figure 4*, the outer region, Ω_2, is modeled using these elements with the shape functions derived from the analytical boundary

series solutions as

o 16-noded IE ($0 \le \xi < \infty$, $-1 \le \eta, \zeta \le 1$):

$$\{N^e\} = \begin{Bmatrix} N_a(\xi)\{\bar{N}(\eta,\zeta)\} \\ N_b(\xi)\{\bar{N}(\eta,\zeta)\} \end{Bmatrix} \quad (22)$$

o 6-noded IE ($0 \le \xi < \infty$):

$$\{N^e\} = \begin{Bmatrix} N_a(\xi)\{\bar{N}(\eta)\} \\ N_b(\xi)\{\bar{N}(\eta)\} \end{Bmatrix} \quad (23)$$

o 6-noded FBBIE
($0 \le \xi < \infty$, $-1 \le \eta \le 1$, $-1 \le \zeta \le 0$):

$$\{N^e\} = \frac{\cosh[k_0(d-d_f)(1+\zeta)]}{\cosh[k_0(d-d_f)]} \begin{Bmatrix} N_a(\xi)\{\bar{N}(\eta)\} \\ N_b(\xi)\{\bar{N}(\eta)\} \end{Bmatrix} \quad (24)$$

in which $\{\bar{N}(\eta,\zeta)\}$ and $\{\bar{N}(\eta)\}$ = the vector of the Lagrange shape functions. $N_a(\xi)$ and $N_b(\xi)$ are the shape functions in the radial(ξ) direction as

$$\begin{Bmatrix} N_a(\xi) \\ N_b(\xi) \end{Bmatrix} = [F]^T \begin{Bmatrix} f_0(\xi) \\ f_1(\xi) \end{Bmatrix} \quad (25)$$

in which $f_0(\xi)$ and $f_1(\xi)$ represent the asymptotic behaviors of the progressive and the first evanescent wave components in the radial direction, respectively, and $[F]$ is the 2×2 coefficient matrix associated with those wave components, which are given by

$$f_0(\xi) = \frac{1}{\sqrt{\xi + r_a}} e^{ik_0(\xi+r_a)-\epsilon\xi} \quad (26)$$

$$f_1(\xi) = \frac{1}{\sqrt{\xi + r_a}} e^{-k_1(\xi+r_a)} \quad (27)$$

$$[F] = \begin{bmatrix} \frac{1}{\sqrt{r_a}} e^{ik_0 r_a} & \frac{1}{\sqrt{r_a}} e^{-k_1 r_a} \\ \frac{1}{\sqrt{r_b}} e^{ik_0 r_b} & \frac{1}{\sqrt{r_b}} e^{-k_1 r_b} \end{bmatrix}^{-1} \quad (28)$$

and ϵ = the artificial damping parameter ($0 < \epsilon \ll k_1$), k_1 = the wave number for the first evanescent wave component, and r_a and r_b = the radial distances to the inner and outer nodes of the infinite elements from the origin as shown in *Figure 4*. The artificial damping parameter(ϵ) in equation (26) has been introduced, to make the integration in equation (17) in the radial(ξ) direction bounded. After the integration is completed analytically, the value of ϵ is taken to be zero. The shape functions, $N_a(\xi)$ and $N_b(\xi)$ in equation (25), except for the artificial damping parameter(ϵ), have been derived from the asymptotic expressions for the progressive and the first evanescent wave components in the analytical boundary series solutions such as

$$\phi_j \approx a_0 \frac{1}{\sqrt{r}} e^{ik_0 r} + a_1 \frac{1}{\sqrt{r}} e^{-k_1 r} \quad (29)$$

It is noted that the corresponding shape functions satisfy the radiation condition at infinity.

The system matrix for the infinite element is constructed by performing the integration in the infinite direction analytically, so that computational efficiency may be acheived.

5. Numerical results and discussions

A three dimensional finite element computer program incorporating the infinite and the fictitious bottom boun ary elements has been developed, and applied to several floating structures in order to illustrate its validity. The accuracy and efficiency of the algorithm depend on the location of the interface between the inner finite element and the outer infinite element regions, and the distance to the fictitious bottom boundary elements from the body surface. The numerical experiments were performed to determine the criteria for the proper distance to the infinite and the fictitious bottom boundary elements using an axisymmetric finite element formulation by the present authors in the previous study[17]. The numerical results indicated that the distance to the infinite elements should be greater than 0.3 times of the incident wave length, and the distance to the fictitious bottom boundary elements should be greater than 0.15 times of the incident wave length from the body surface. In this study, using those criteria, the example analyses are carried out for the floating square barges in finite and infinite depths.

Floating square Barge in finite depth

Figure 6 presents the analysis results for a floating square barge with $h/a = 0.5$, $d/a = 1.0$, and $\psi = 0°$ (*Figure 8(a)*), in which a and h = the half width and the draft of the barge, d = the depth of water, and ψ = the angle of the incident wave attack. Unlike the previous examples, this case must be treated solely as a three dimensional problem. Yue *et al.*[10,11] reported the results for the case of a fixed barge (i.e., diffraction problem) by using a hybrid element method (HEM).

In this study, the diffraction and radiation problems are analyzed by using the element grid system with 371 nodes. The exciting force coefficients and the added mass and damping coefficients are calculated for various frequencies, and given in *Figures 6(b)* and *(c)*, respectively. *Figure 6(b)* indicates that the present method gives satisfactory results compared with those using a hybrid element method by Yue *et al.*

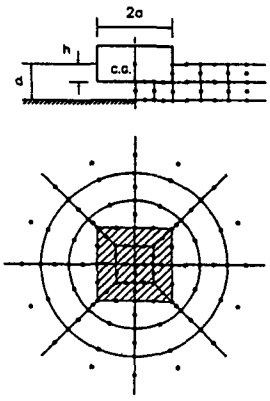

(a) Geometry and element meshes

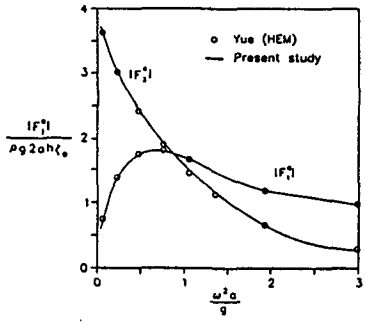

(b) Horizontal and vertical force coefficients

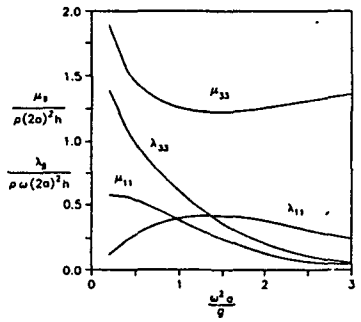

(c) Added mass and damping coefficients

Figure 6 Results for a floating square barge with $h/a = 0.5$, $d/a = 1.0$, and $\psi = 0°$

Floating square barge in infinite depth

Figure 7 presents the surge and the heave responses for a floating square barge with $h/a = 8/9$, $d/a = \infty$, and $\psi = 0°$. The fluid domain is modeled by using the element grid system with 633 nodes as shown in *Figure 7(a)*. The present results are compared with those obtained using a three dimensional Green's function by Garrison[19], and also with experimental results by Faltinsen *et al.*[20]. It is found that the present method incorporating the infinite and the fictitious bottom boundary elements gives the satisfactory results except for the slight discrepancy of the resonance frequency for the heave motion. The discrepancy is caused by the differences of the heave added mass coefficients (μ_{33}) between the present results and the published results by Garrison. The heave added mass coefficients (μ_{33}) obtained in this study are found to be smaller than those of Garrison approximately by 10%. The differences might be caused by the shape functions of the fictitious bottom boundary element in the vertical direction (see, equation (20)) employed in this study. Further study is needed to investigate the cause of the discrepancy.

6. Conclusions

In this paper, the finite element technique incorporating infinite elements is applied to analyzing the general

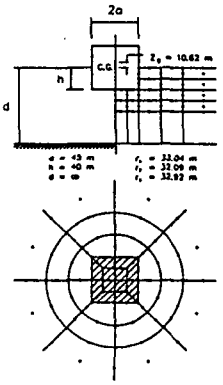

(a) Geometry and element meshes

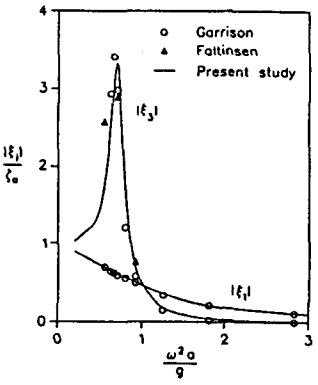

(b) Surge ($|\xi_1|$) and heave ($|\xi_3|$) responses

Figure 7 Hydrodynamic responses of a floating square barge with $h/a = 8/9$, $d/a = \infty$, and $\psi = 0°$

three dimensional wave–structure interaction problems. Two types of elements are developed to discretize the fluid domain efficiently. One is the infinite element for modeling the radiation condition at infinity, and the other is the fictitious bottom boundary element for an efficient discretization of the fluid domain for the case of deep water. The shape functions for the infinite element, in the radial direction, are derived from the asymptotic expressions for the progressive wave and the evanescent wave components in the analytical boundary series solutions.

Verification of the elements developed in this study is carried out utilizing several kinds of floating structures. Comparisons with the results from other available solution methods and experimental data indicate that the present method incorporating the infinite and the fictitious bottom boundary elements gives good results.

References

1. John, F. On the motion of floating bodies II. *Comm. Pure Appl. Math.* 1950, **3**, 45–101
2. Mei, C.C. Numerical methods in water–wave diffraction and radiation. *Ann. Rev. Fluid Mech.* 1978, **10**, 393–416
3. Zienkiewicz, O.C., Bettess, P. and Kelly, D.W. The finite element method for determining fluid loading on rigid structures, two– and three–dimensional formulations. *Numerical methods in offshore engineering*, Zienkiewicz, O.C. *et al.*, eds., Wiley, Chichester, England, 1978, 141–183
4. Bai, K.J. A variational method in potential flows with a free surface. Univ. of California, Berkeley, College of Engineering, Report No. NA72-2, 1972
5. Huang, M.C., Leonard, J.W. and Hudspeth, R.T. Wave interference effects by finite element method. *J. Waterway, Port, Coastal, and Ocean Div.*, ASCE 1985, **111**, No.1, 1–17
6. Huang, M.C., Hudspeth, R.T. and Leonard, J.W. FEM solution 3–D wave interference problems. *J. Waterway, Port, Coastal, and Ocean Div.*, ASCE 1985, **111**, No.4, 661–677
7. Sharan, S.K. Modelling of radiation damping in fluids by finite elements. *Int. J. Numer. Meth. Engng* 1986, **23**, 945–957
8. Sharan, S.K. Hydrodynamic loadings due to the motion of large offshore structures. *Comput. Struct.* 1989, **32**, No.6, 1211–1216
9. Bai, K.J. and Yeung, R.W. Numerical solution to free–surface flow problems. *The 10th Symposium of Naval Hydrodynamics*, 1974, Office of Naval Research, Cambridge, Massachusetts, 609–647
10. Yue, D.K.P., Chen, H.S. and Mei, C.C. A hybrid element method for calculating three–dimensional water wave scattering. *Technical Report No.215* 1976, Ralph M. Parsons Laboratory for Water Resources and Hydrodynamics, Dept. of Civil Engineering, M.I.T. Cambridge, Mass.
11. Yue, D.K.P., Chen, H.S. and Mei, C.C. A hybrid element method for diffraction of water waves by three–dimensional bodies. *Int. J. Numer. Meth. Engng* 1978, **12**, 245–266
12. Taylor, R.E. and Zietsman, J. A comparison of localized finite element formulations for two–dimensional wave diffraction and radiation problems. *Int. J. Numer. Meth. Engng* 1981, **17**, 1355–1384
13. Zienkiewicz, O.C., Kelly, D.W. and Bettess, P. The coupling of the finite element method and boundary solution procedures. *Int. J. Numer. Meth. Engng* 1977, **11**, 355–375
14. Bettess, P. and Zienkiewicz, O.C. Diffraction and refraction of surface waves using finite and infinite elements. *Int. J. Numer. Meth. Engng* 1977, **11**, 1271–1290
15. Zienkiewicz, O.C., Bando, K., Bettess, P., Emson, C. and Chiam, T.C. Mapped infinite elements for exterior wave problems. *Int. J. Numer. Meth. Engng* 1985, **21**, 1229–1251
16. Lau, S.L. and Ji, Z. An efficient 3–D infinite element for water wave diffraction problems. *Int. J. Numer. Meth. Engng* 1989, **28**, 1371–1387
17. Park, W–S. and Yun, C–B. Infinite elements for diffraction and radiation problems of water waves. *Proc. the First Pacific/Asia Offshore Mech. Symp.* 1990, **2**, 17–23
18. Sommerfeld, A. *Partial differential equations in physics.* Academic Press, New York, 1949
19. Garrison, C.J. Hydrodynamic interaction of waves with a large displacement floating body. Naval Postgraduate School, Monterey, CA 93940, Report No. NPS–69Gm77091 1977
20. Faltinsen, O.M. and Michelsen, F.C. Motion of large structures in waves at zero Froude number. *The Dynamics of Marine Vehicles and Structures in Waves* 1974, Paper No. 11, 91–106